Activating an adaptive immune response from a hydrogel scaffold imparts regenerative wound healing.

Donald R. Griffin[1,2†], Maani M. Archang[3†], Chen-Hsiang Kuan[4,5,6], Westbrook M. Weaver[3,&], Jason S. Weinstein[7], An Chieh Feng[8], Amber Ruccia[8], Elias Sideris[1], Vasileios Ragkousis[8], Jaekyung Koh[3], Maksim V. Plikus[4,5,10,11], Dino Di Carlo[3], Tatiana Segura[3,6*], Philip O. Scumpia[8,12*]

1. Chemical and Biomolecular Engineering Department, University of California, Los Angeles, Los Angeles, CA
2. Biomedical Engineering, Chemical Engineering, University of Virginia, Charlottesville, VA
3. Bioengineering Department, University of California, Los Angeles, Los Angeles, CA
4. Department of Developmental and Cell Biology, University of California, Irvine, CA
5. Sue and Bill Gross Stem Cell Research Center, University of California, Irvine, Irvine, CA
6. Division of Plastic Surgery, Department of Surgery, National Taiwan University Hospital, Taipei, Taiwan
7. Department of Medicine, Rutgers –New Jersey Medical School, Newark, NJ
8. Division of Dermatology, Department of Medicine, David Geffen School of Medicine, University of California, Los Angeles, Los Angeles, CA
9. Departments of Biomedical Engineering, Neurology, Dermatology Duke University, Durham NC,
10. Center for Complex Biological Systems, University of California, Irvine, Irvine, CA
11. NSF-Simons Center for Multiscale Cell Fate Research, University of California-Irvine, Irvine, CA
12. Department of Dermatology, VA Greater Los Angeles Healthcare System-West Los Angeles, Los Angeles, California

† Donald R. Griffin and Maani M. Archang contributed equally to this work.

& Current address Tempo Therapeutics, San Diego, CA 92109

* To whom correspondence should be addressed

Philip O. Scumpia
PScumpia@mednet.ucla.edu

Tatiana Segura
Tatiana.segura@duke.edu

Supplementary Figures

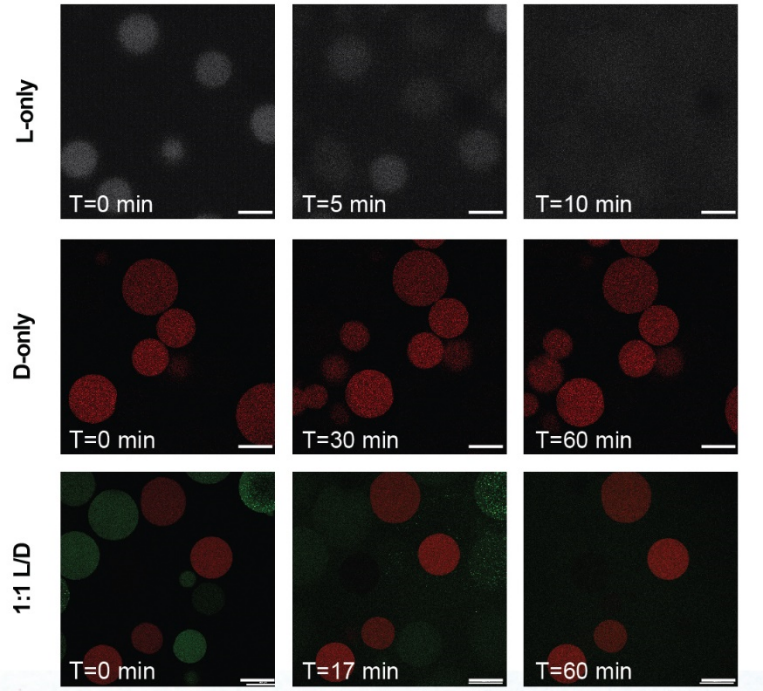

Supplementary Figure 1. In vitro characterization of L- and D- chiral microparticles and MAP hydrogel: Collagenase I degradation study of L, D and a 1:1 mixture of L and D microgels. As expected, L-peptide crosslinked microgels are degradable by collagenase I and are completely degraded by 60 minutes. I contrast D-peptide crosslinked microgels have no visible degradation within the 60-minute incubation in collagenase I. In a 1:1 mixture of L and D-peptide crosslinked microgels only L-peptide crosslinked microgels degrade. Images show representative examples of microscope images from in vitro hydrogel degradation of L, D, and 1:1 L/D-MAP. Scale = 200µm.

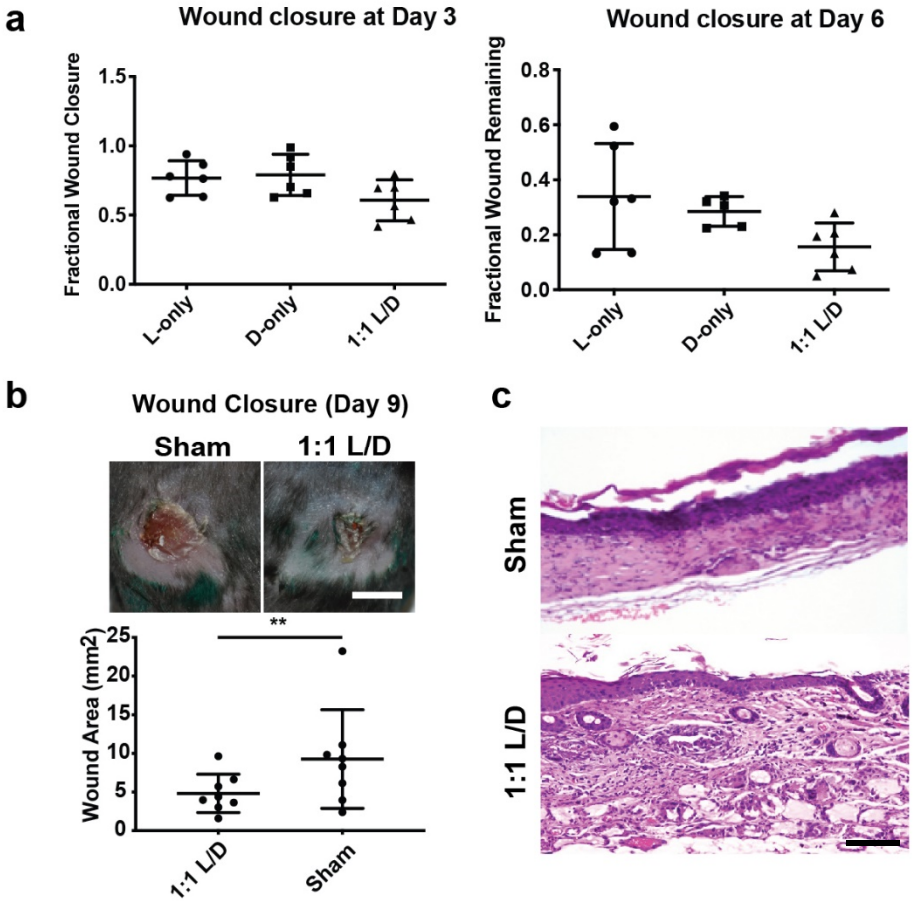

Supplementary Figure 2. Early wound closure results with different hydrogel treatments. a) No difference in wound closure between different L, D, and L/D MAP hydrogel treatment. n = 6 B6 mice, mean +/- SD. **b)** Comparison of L and D hydrogel to sham in B6 mice at day 9 reveals improved wound closure when compared to Sham. n = 8 B6 mice, mean +/- SD. Scale = 5mm. ** denotes two-tailed p=0.0078 by Wilcoxon matched pair signed rank test. **c)** 100x view of histology from SKH1 (hairless) mice 21 days after wounding demonstrating typical scar formation in sham mice (top) or vellus hair follicles and sebaceous glands directly over several degrading MAP gel particles in a mouse that was treated with D-MAP hydrogel. Scale = 100µm.

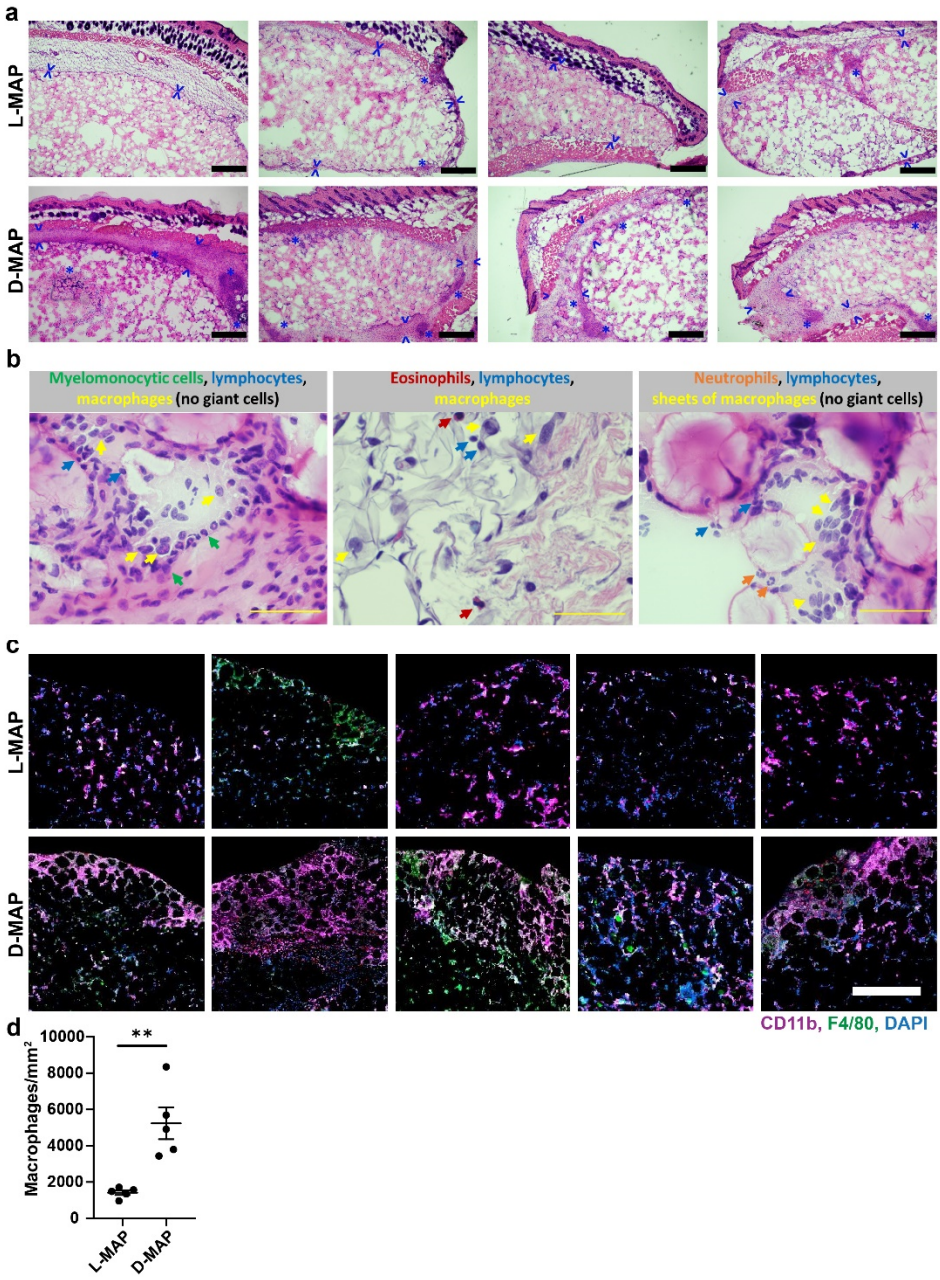

Supplementary Figure 3. Characterization of subcutaneous MAP implants. a) H&E staining of subcutaneous implants of L-MAP and D-MAP hydrogels. Arrowheads denote the expansion of the fibrous capsule with lymphohistiocytic cells and with admixed neutrophils and eosinophils. Asterisks denote foci of more robust inflammation. Note the minimal fibrous capsule and inflammatory response in L-MAP hydrogels compared to more robust response in D-MAP. Scale = 500µm **b)** Representative high-resolution H&E staining micrographs of subcutaneous D-MAP implants showing the macrophages, lymphocytes, and scattered eosinophils and neutrophils. Scale = 50 µm **c)** Immunofluorescence images from all subcutaneous implants of L-MAP and D-MAP hydrogels for F4/80 (green), CD11b (purple), IL-33 (red), and DAPI (blue). White to light pink denotes co-staining for F4/80 and CD11b antigens. Scale = 500 µm. (a) and (b,c) represent separate experiments. **d)** Quantification of $F4/80^{+}CD11b^{+}$ macrophages in the edge of L-MAP and D-MAP implants. ** denotes p=0.0025 on two-tailed unpaired T test. n = 5 B6 mice (whole hydrogels analysis), mean +/- SEM.

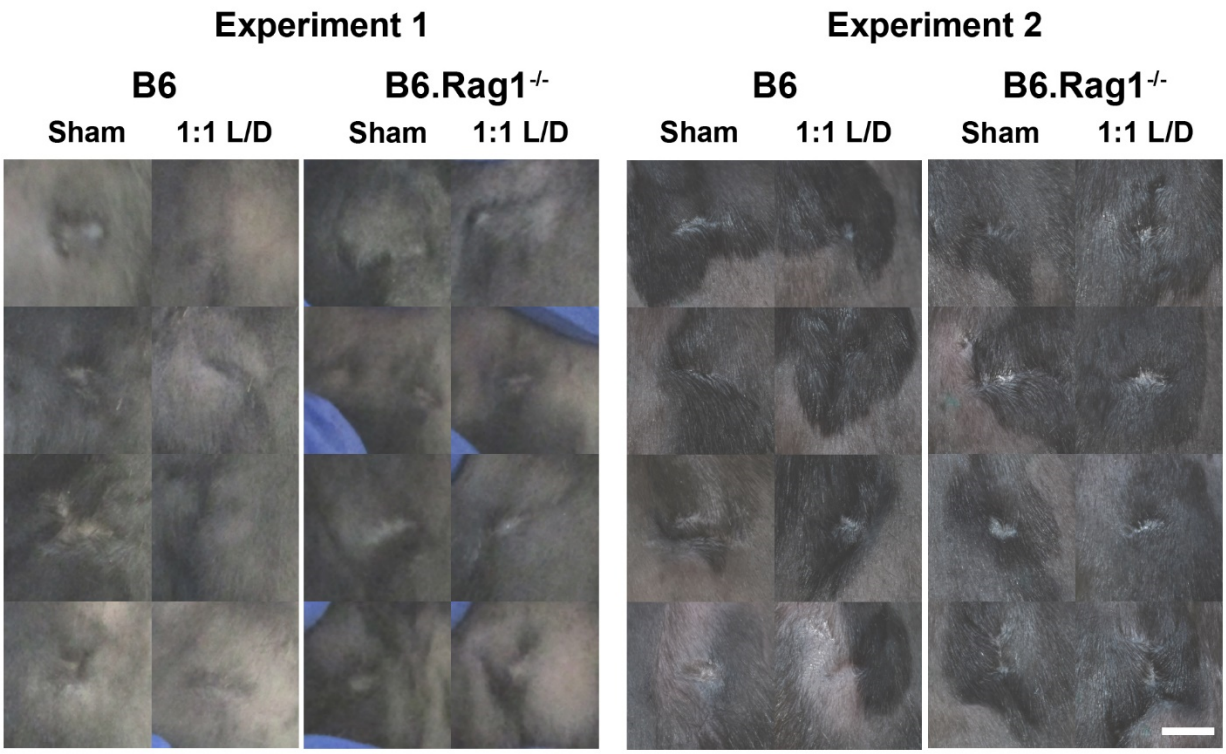

Supplementary Figure 4. L/D MAP hydrogel diminishes the clinical appearance of scar in WT mice but not B6.Rag1$^{-/-}$ mice. Splinted wounds (6mm) were performed on B6 or B6.Rag1$^{-/-}$ mice, and one side was treated with L/D MAP hydrogel and the other with no hydrogel. On Day 16, clinical photographs of wounds were taken. Shown are all healed wounds, paired by mouse, in two separate experiments. Scale = 2mm.

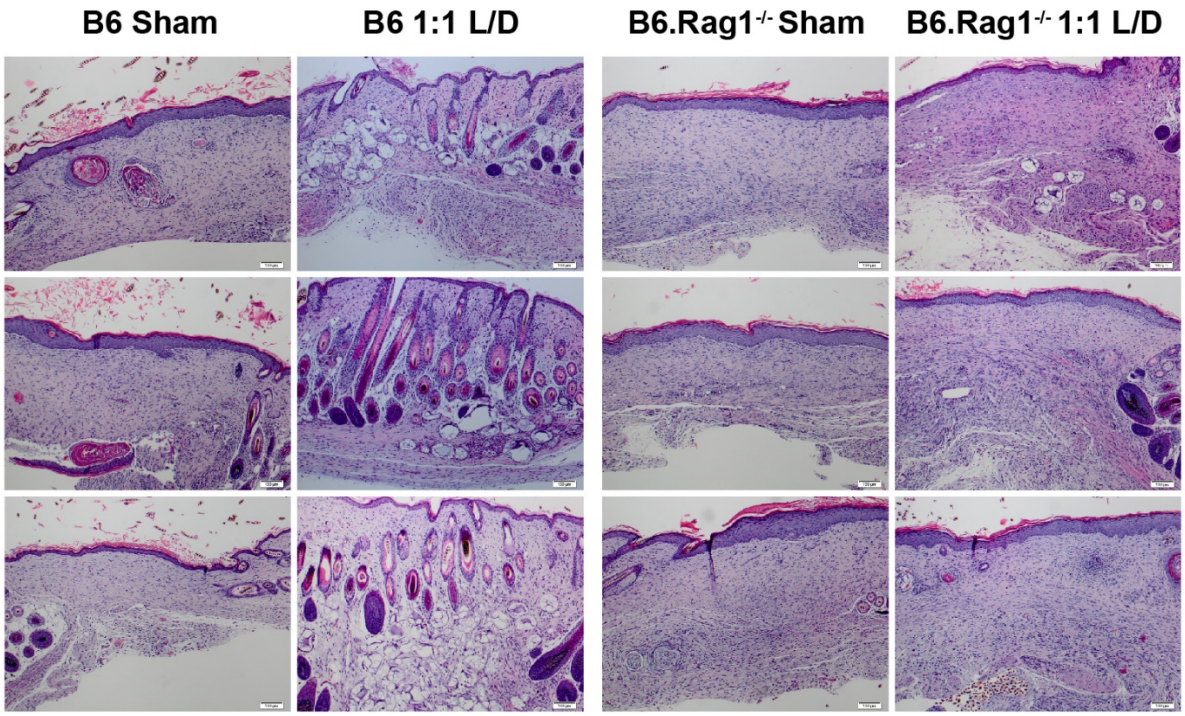

Supplementary Figure 5. Additional histology from healed 1:1 L/D-MAP or Sham treated wounds, B6 mice, and B6.Rag1$^{-/-}$ mice. Note in the 1:1 L/D-MAP treated B6 samples, multiple hair follicles and some sebaceous glands, including some in disarrayed orientation compared to the surrounding tissue, are present directly overlying degrading microgels. Similar hair follicles are not present in any other group of samples. n = 3 per group shown. Scale = 100µm.

Supplementary Discussion

To further characterize how D-MAP enhances innate immune recruitment, we evaluated histology of subcutaneous implants. After 21 days, L- or D-MAP implants were removed from the mice. As we previously demonstrated[1], most L-MAP implants did not display traditional fibrous capsule formation and only a few areas displayed some focal and thin fibrous capsules containing small foci of immune cells (Supplementary Figure 3a). No foreign body reaction with giant cells were noted within or surrounding the hydrogel, but some lymphohistiocytic immune infiltrates were seen dispersed randomly within and in areas towards the edge of the implant (Supplementary Figure 3a). This is likely a property of the hyperporous nature of the MAP hydrogel allowing cells to migrate through the hydrogel rather than typical materials that allow a build-up of immune cells at the edges of the hydrogel. In contrast, D-MAP implants displayed thick fibrous capsules filled with mainly lymphohistiocytic cells and rare scattered neutrophils and eosinophils (Supplementary Figure 3a-c). Epithelioid histiocytes degrading hydrogel particles with scattered surrounding lymphocytes, and rare eosinophils and neutrophils were detected at the edges of the scaffold. Many more of these immune aggregates were found within D-MAP scaffolds than L-MAP scaffolds (denoted by *s in Supplementary Figure 3a). These findings are not consistent with a typical type 1 foreign body granuloma (no foreign body giant cells with sheaths of surrounding lymphocytes) associated with a strong Th1/M1 immune response seen in tuberculosis or with inflammatory materials. Instead, the material was eliciting a type II foreign body reaction typically associated inert foreign materials such as silicone[2–4]. Immunofluorescent staining for F4/80 and CD11b confirmed the increased presence of $F4/80^{+}CD11b^{+}$ macrophages within the D-MAP scaffolds at 21 days with concentrations at the edges of the hydrogel (Supplementary Figures 3b and 3c). These data suggest that D-MAP either possesses increased adjuvant properties by itself, or the MAP hydrogel itself that is being amplified by the presence of D-chiral peptides or the MAP hydrogel possesses adjuvant properties and the presence of D-chiral peptides induce an adaptive immune response that can dramatically amplify the immune response to the MAP hydrogel.

Supplementary References

1. Koh, J. *et al.* Enhanced In Vivo Delivery of Stem Cells using Microporous Annealed Particle Scaffolds. *Small Weinh. Bergstr. Ger.* **15**, e1903147 (2019).
2. Warren, K. S. A functional classification of granulomatous inflammation. *Ann. N. Y. Acad. Sci.* **278**, 7–18 (1976).
3. Chensue, S. W. *et al.* Cytokine responses during mycobacterial and schistosomal antigen-induced pulmonary granuloma formation. Production of Th1 and Th2 cytokines and relative contribution of tumor necrosis factor. *Am. J. Pathol.* **145**, 1105–1113 (1994).
4. Ellis, L. Z., Cohen, J. L. & High, W. Granulomatous reaction to silicone injection. *J. Clin. Aesthetic Dermatol.* **5**, 44–47 (2012).